

# Differential effects of insulin signaling on individual carbon fluxes for fatty acid synthesis in brown adipocytes

Hyuntae Yoo\*, Maciek Antoniewicz<sup>†</sup>, Joanne K. Kelleher<sup>†</sup>, and Gregory Stephanopoulos<sup>†</sup>  
Departments of Chemistry\* and Chemical Engineering<sup>†</sup>, Massachusetts Institute of Technology,  
Cambridge, MA 02139, U.S.A.

**Abstract**— Considering the major role of insulin signaling on fatty acid synthesis via stimulation of lipogenic enzymes, differential effects of insulin signaling on individual carbon fluxes for fatty acid synthesis have been investigated by comparing the individual lipogenic fluxes in WT and IRS-1 knockout (IRS-1 KO) brown adipocytes. Results from experiments on WT and IRS-1 KO cells incubated with [<sup>5-<sup>13</sup>C</sup>] glutamine were consistent with the existence of reductive carboxylation pathway. Analysis of isotopomer distribution of nine metabolites related to the lipogenic routes from glucose and glutamine in IRS-1 KO cells using [U-<sup>13</sup>C] glutamine as compared to that in WT cells indicated that flux through reductive carboxylation pathway was diminished while flux through conventional TCA cycle was stimulated due to absence of insulin signaling in IRS-1 KO cells. This observation was confirmed by quantitative estimation of individual lipogenic fluxes in IRS-1 KO cells and their comparison with fluxes in WT cells. Thus, these results suggest that glutamine's substantial contribution to fatty acid synthesis can be directly manipulated by controlling the flux through reductive carboxylation of alpha-ketoglutarate to citrate using hormone (insulin).

**Index Terms** — brown adipocyte, fatty acid synthesis, insulin signaling, and reductive carboxylation pathway

## I. INTRODUCTION

**O**BESITY and type II diabetes are among the most widespread and high-cost epidemics with rapid increase in the incidents for the last decade. There have been evidences that excessive fat synthesis in obesity may give rise to elevated free fatty acids, which in turn could lead to hepatic insulin resistance, one of the major early

events of type II diabetes [1]. Therefore, understanding the detailed mechanism of regulation for fat synthesis and its relationship with insulin signaling may provide insights into the pathogenesis of the two diseases and help preventing them.

Insulin signaling has long been associated with elevating overall lipogenic activity through increased activity of lipogenic enzymes [2]. Evidences have been accumulated that many of these enzymes are stimulated directly by insulin signaling via insulin response element at their transcription level or indirectly by insulin signaling to transcription factors [3]. However, studies on stimulation of lipogenic enzymes' activity by insulin signaling have been largely limited to the enzymes directly related to glucose's metabolic route to fatty acid synthesis, namely

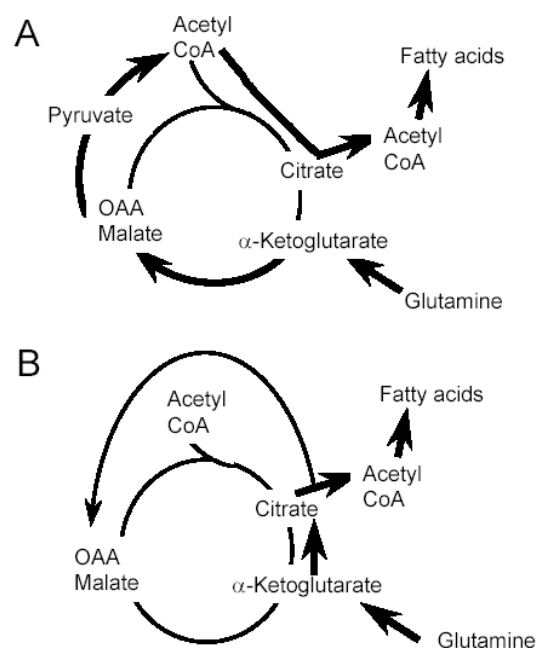


Fig. 1. Two pathways for glutamine's metabolic route to fatty acid synthesis. A. Glutaminolysis pathway. Glutamine enters TCA cycle at  $\alpha$ -ketoglutarate and converted to succinate, fumarate, and malate, whose further conversion to pyruvate and acetyl-CoA leads to fatty acid synthesis. B. Reductive carboxylation pathway. Glutamine enters TCA cycle at  $\alpha$ -ketoglutarate, which is directly converted to isocitrate and citrate via reductive carboxylation and cleaved to supply acetyl-CoA for fatty acid synthesis.

Manuscript received November 19, 2004. This work was supported in part by National Institute of Health Grant DK-58533.

H. Yoo is with the Massachusetts Institute of Technology, Cambridge, MA 02139 USA (e-mail: htdino@mit.edu).

M. Antoniewicz is with the Massachusetts Institute of Technology, Cambridge, MA 02139 USA (e-mail: maciek@mit.edu).

J. K. Kelleher is with Department of Chemical Engineering, Massachusetts Institute of Technology, Cambridge, MA 02139 USA. (e-mail: jkk@mit.edu).

G. Stephanopoulos is with Department of Chemical Engineering, Massachusetts Institute of Technology, Cambridge, MA 02139 USA. (corresponding author - phone: 617- 253-4583; fax: 617-253-3122; e-mail: [gregstep@mit.edu](mailto:gregstep@mit.edu)).

glucose transporter, glucokinase, glyceraldehyde-3-phosphate dehydrogenase, ATP-citrate lyase, acetyl-CoA carboxylase, fatty acid synthase, and malic enzyme (as supplier of NADPH for fatty acid synthesis). The effect of insulin on enzymes for lipogenic utilization of other carbon sources has been neglected because their contribution was thought to be minimal. Moreover, analysis of the lipogenic fluxes from glucose to fatty acid synthesis has been qualitative, examining only the overall lipogenic activity and not the individual fluxes.

Among alternative carbon sources for lipogenesis, glutamine has attracted some attention because its considerable contribution to lipogenesis in many mammalian tissues was shown by significant incorporation of  $^{14}\text{C}$ -label from  $^{14}\text{C}$ -glutamine into triglyceride [4-6]. In wild-type brown adipocytes, glutamine's contribution to *de novo* synthesis of fatty acids has been shown to be higher than that of glucose in our previous report [7]. In this report, we also showed that in insulin receptor substrate-1 knockout (IRS-1 KO) brown adipocytes glutamine's fractional contribution to fatty acid synthesis was much lower than that of glucose. It has been demonstrated that phosphatidylinositol 3-kinase (PI3K)-mediated insulin-

signaling pathway was greatly impaired in IRS-1 KO brown adipocytes [8][9]. Thus, utilization of glutamine as lipogenic carbon source may be regulated by insulin signaling to a stronger extent than that of glucose in brown adipocytes.

In this study, the two possible pathways for glutamine's metabolic route to fatty acid synthesis (Fig. 1) have been examined in both WT and IRS-1 KO brown adipocytes by  $[5-^{13}\text{C}]$  glutamine. Using the isotopomer distribution data for nine lipogenesis-related metabolites from incubation with  $[\text{U}-^{13}\text{C}]$ -labeled glutamine, we have quantitatively analyzed the individual fluxes that make up the lipogenic routes from glucose and glutamine as two major carbon sources in WT and IRS-1 KO brown adipocytes. Comparison of individual fluxes in WT and IRS-1 KO cells confirmed the importance of glutamine as lipogenic carbon source in brown adipocytes. Moreover, the potential sites for regulating glutamine's lipogenic flux by insulin signaling were identified.

## II. EXPERIMENTAL PROCEDURES

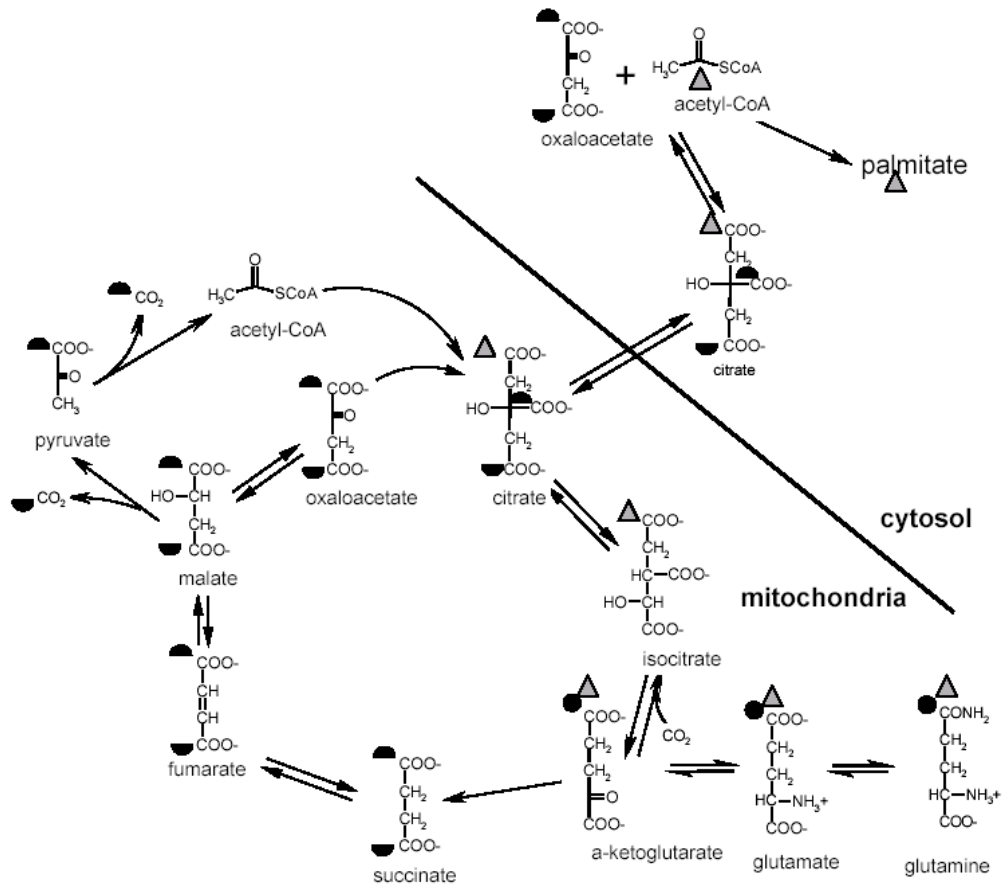


Fig. 1. Metabolic network scheme to distinguish the two pathways for glutamine's route to fatty acid synthesis, using  $[5-^{13}\text{C}]$  glutamine.

If glutamine follows glutaminolysis pathway,  $^{13}\text{C}$ -label at C-5 of glutamine will be found in either of the two terminal carbons of succinate because of its symmetry. Both  $^{13}\text{C}$ -labels will then be lost as  $\text{CO}_2$  when malate is converted to pyruvate and acetyl-CoA.  $^{13}\text{C}$ -labels on the two terminal carbons of oxaloacetate will not be transferred to acetyl-CoA when citrate is cleaved to oxaloacetate plus acetyl-CoA, because of the stereospecificity of ATP-citrate lyase. If glutamine follows reductive carboxylation pathway,  $^{13}\text{C}$ -label at C-5 of glutamine will be maintained at acetyl-CoA side of the terminal carbon of citrate. When citrate is cleaved by ATP-citrate lyase,  $^{13}\text{C}$ -label is transferred to acetyl-CoA and incorporated into fatty acid synthesis.

### A. Materials

Biochemicals were obtained from Sigma Chemical Co., St. Louis, MO.  $^{13}\text{C}$ -labeled chemicals were obtained from Cambridge Isotope Laboratories, Inc., Andover, MA. Tissue culture media were obtained from Invitrogen, Co., Carlsbad, CA.

### B. Cell cultures and adipocyte differentiation

Brown adipocyte cells were cultured with the same procedure as in Yoo *et al.* [7] Briefly, WT and IRS-1 KO brown preadipocytes were grown in 6-well plates (surface area =  $10\text{ cm}^2$ ) to confluence in differentiation media containing 25 mM glucose, 4 mM glutamine, 20 nM insulin, 1 nM T3, and 10 % fetal bovine serum as well as 44 mM  $\text{NaHCO}_3$  (day 0). The media were then replaced with fresh induction media, which was differentiation media plus 0.125 mM indomethacin, 0.25 mM IBMX, and 5  $\mu\text{M}$  dexamethasone. On day 2 and day 4, the media were replaced with fresh differentiation media to reach day 6. In  $[5\text{-}^{13}\text{C}]$  glutamine experiment, the media from day 2 to day 6 contained 4 mM  $[5\text{-}^{13}\text{C}]$  glutamine and 25 mM unlabeled glucose. In studies for the determination of carbon flux from glucose or glutamine to fatty acid synthesis through tricarboxylic acid (TCA) cycle, on day 4 the media were changed to differentiation media without glucose or glutamine at 42 hrs after day 2. The differentiation media were supplemented with selected concentration of oxalomalate or 2-methylisocitrate and incubated at  $37^\circ\text{C}$  for 10 min, followed by addition of glucose and glutamine with specified  $^{13}\text{C}$ -labeling. In six hours, cells were harvested for analysis of metabolites.

### C. Isolation and derivatization of organic/amino acids and lipids

For isolation of organic/amino acids, the procedure described in Fiehn *et al.* [20] was modified as follows. 0.7 mL methanol and 25  $\mu\text{L}$  water was added to each well of 6-well plate immediately after removal of the media. In 15 min after incubation at room temperature, methanol extract was mixed with 0.7 mL water and 0.37 mL chloroform in 15 mL tube. Vigorous vortexing was followed by centrifugation at  $3000 \times g$  for 3 min. The chloroform layer was carefully removed and the methanol/water layer was centrifuged again at  $3000 \times g$  for 3 min. Clear solution of methanol/water layer (separated from white precipitate) was then transferred to glass vial and evaporated. The residue was dissolved in 70  $\mu\text{L}$  of methoxyamine hydrochloride (20 mg/mL in pyridine) and vortexed. After 90 min incubation at  $37^\circ\text{C}$ , organic/amino acids were derivatized with 70  $\mu\text{L}$  of N-methyl-N-*tert*-butyldimethylsilyltrifluoroacetamide (MTBSTFA) at  $70^\circ\text{C}$  for 30 min. The reaction mixture was then directly injected into GC-MS instrument for analysis of the isotopomer distribution of organic/amino acids. Isolation of lipids and derivatization of palmitate moiety into methyl ester were performed as described previously [7].

### D. GC-MS for isotopomer distribution measurement

Samples from  $[5\text{-}^{13}\text{C}]$  glutamine experiment were analyzed for palmitate isotopomer distribution with the same instrumental setup as previously reported [7]. The samples from the rest of the experiments were analyzed with another GC-MS instrument described below. Isotopomer distributions of fatty acid methyl esters measured with the second GC-MS instrument with scan mode were essentially identical to those measured with the first GC-MS with selected ion monitoring (SIM) mode.

Samples were injected into a Hewlett-Packard model 5890 series II Gas Chromatograph connected to HP5971 series Mass Selective Detector and equipped with DB-XLB (60 m x 0.25 mm id x 0.25 mm) capillary column (J&W Scientific, Folsom, CA). Helium flow with 10 psi inlet pressure was maintained by electronic control. The temperatures of the injector and the detector were kept at  $230^\circ\text{C}$  and  $300^\circ\text{C}$ , respectively. For isotopomer distribution analysis of methyl palmitate and its isotopomers (M+0 to M+16 ( $m/z=270$  to  $286$ )), GC column temperature was started at  $100^\circ\text{C}$  and held for 1 min. The temperature was then increased to  $250^\circ\text{C}$  at  $10^\circ\text{C}/\text{min}$ , and held for 5 min. It was increased to  $300^\circ\text{C}$  at  $25^\circ\text{C}/\text{min}$  and held for 2 min. Mass range of 100 to 350 was recorded at 2.7 scans per second. For isotopomer distribution analysis of acid derivatives, GC temperature was started at  $100^\circ\text{C}$  and held for 5 min. The temperature was then increased to  $300^\circ\text{C}$  at  $10^\circ\text{C}/\text{min}$ , and held for 5 min. Mass range of 50 to 550 was recorded at 1.5 scans per second. The most abundant fragments (M-57) of the following acid derivatives (*tert*-butyldimethylsilyl; TBDMS) were analyzed for their isotopomer distributions: pyruvate ( $m/z=174\text{-}178$ ), lactate ( $m/z=261\text{-}265$ ), fumarate ( $m/z=287\text{-}293$ ),  $\alpha$ -ketoglutarate ( $m/z=346\text{-}354$ ), malate ( $m/z=419\text{-}423$ ), aspartate ( $m/z=418\text{-}424$ ), glutamate ( $m/z=432\text{-}440$ ), and citrate ( $m/z=459\text{-}468$ ).

Uptake fluxes for glucose and glutamine into WT cells were calculated from the rates of consumption of glucose and glutamine from medium as reported previously [7].

### E. Data Analysis

Fractional contribution of  $^{13}\text{C}$ -labeled carbon sources to fatty acid synthesis (D value) and fractional new synthesis of fatty acids during time  $t$  ( $g(t)$  value) were estimated with the isotopomer distribution measurements of palmitate based on the model of isotopomer spectral analysis (ISA) as reported previously [7]. For estimation of fluxes in the metabolic network model (Fig. 5) by integrating the isotopomer distributions of palmitate, pyruvate, lactate, fumarate,  $\alpha$ -ketoglutarate, malate, aspartate, glutamate, and citrate, a MATLAB program was used. Based on steady-state assumption, the program estimates fluxes for reactions in the metabolic network model that fit the inputs of a metabolic network (consisting of a set of reactions, each with specific atomic transitions between defined metabolites) and measurements of isotopomer distributions of some metabolites, using least-square fit method. Given

measurement errors for the isotopomer distribution data, the program can calculate how good the fit for each metabolite's measurement is and the uncertainty of each estimated flux.

Glucose and glutamine taken up from medium and preexisting palmitate were defined as substrates, and production of lactate (exported into medium), palmitate, and protein synthesis from aspartate was treated as sink. The rest of the metabolites were regarded as balanced except for CO<sub>2</sub>, which was allowed to be unbalanced.

The equations for the whole metabolic network were set up with 32 variables (fluxes). The number of independent measurements for solving the equations was 50, the sum of “the number of isotopomers – 1” for nine metabolites. Each measurement of isotopomer distribution was corrected for natural abundance by the program before flux estimation.

For each set of flux estimation results, statistical evaluation of how good the fit was for each metabolite's isotopomer distribution was calculated in terms of sum of square residuals (SSRES) based on measurement errors. SSRES was defined as  $\sum$  (difference between data and fit / measurement error)<sup>2</sup>. Overall goodness of fit was calculated by summing up SSRES values for all nine metabolites, which was compared with the range of SSRES values for 95% confidence calculated by the program.

### III. RESULTS

#### A. [5-<sup>13</sup>C] glutamine's contribution to palmitate synthesis in IRS-1 KO brown adipocytes

In order to assess the significance of reductive carboxylation pathway in glutamine's contribution to palmitate synthesis in IRS-1 KO brown adipocytes [7], the incorporation of <sup>13</sup>C from [5-<sup>13</sup>C] glutamine into palmitate synthesis was examined after 4-day incubation of WT and IRS-1 KO cells with 25 mM unlabeled glucose and 4 mM [5-<sup>13</sup>C] glutamine from day 2 to day 6. Substantial incorporation of <sup>13</sup>C from C-5 of glutamine into palmitate (Fig. 1) was also analyzed for fractional contribution of [5-<sup>13</sup>C] glutamine to lipogenic acetyl-CoA by ISA model. [5-

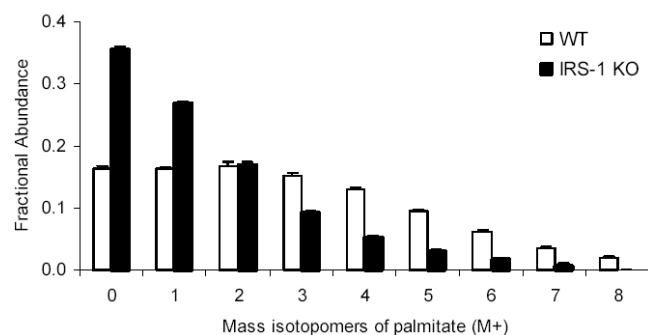


Fig. 2. Contribution of [5-<sup>13</sup>C] glutamine to palmitate synthesis in WT and IRS-1 KO brown adipocytes.

Isotopomer distribution of palmitate isolated from WT and IRS-1 KO brown adipocytes under incubation in media containing 25 mM unlabeled glucose and 4 mM [5-<sup>13</sup>C] glutamine from day 2 to day 6. Data shown are mean  $\pm$  SEM (n = 3).

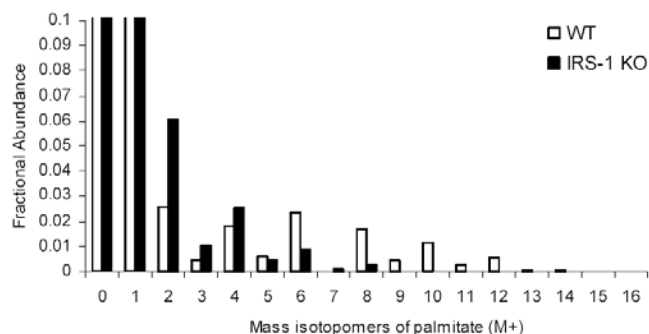


Fig. 3. Differential incorporation of glutamine carbon into palmitate synthesis in WT and IRS-1 KO cells.

Isotopomer distribution of palmitate from WT and IRS-1 brown adipocytes on day 4 under 6-hr incubation in media containing 25 mM unlabeled glucose and 4 mM [U-<sup>13</sup>C] glutamine.

<sup>13</sup>C] glutamine contributed  $34.1 \pm 0.6$  % to palmitate synthesis in WT cells and  $18.5 \pm 0.1$  % in IRS-1 KO cells.

#### B. Isotopomer distribution of nine metabolites related to fatty acid synthesis

Incorporation of glutamine carbon into palmitate synthesis was measured for WT and IRS-1 KO cells, in order to determine the difference in the capacity of glutamine utilization. Incubation of the cells in 25 mM unlabeled glucose and 4 mM [U-<sup>13</sup>C] glutamine for 6 hours on day 4 led to more active utilization of glutamine in WT cells than in IRS-1 KO cells (Fig. 3), consistent with the results from 4-day incubation in our previous report [7] and Figure 2. Eight additional metabolites that are directly related to glutamine's metabolic routes to fatty acid synthesis (glutamate,  $\alpha$ -ketoglutarate, citrate, fumarate, malate, aspartate, pyruvate, and lactate) were also examined in WT and IRS-1 KO cells. After 6-hr incubation in 25 mM unlabeled glucose and 4 mM [U-<sup>13</sup>C] glutamine, isotopomer distribution of the metabolites were measured and compared with those of wild-type cells [12] (Figs. 4A-4H). Isotopomer distribution of glutamate,  $\alpha$ -ketoglutarate and citrate in IRS-1 KO cells were most distinct from that of WT cells in the fractional abundance of M+5 isotopomer. M+4 isotopomers of fumarate, malate, aspartate of IRS-1 KO cells were remarkably higher in fractional abundance than those of WT cells. In contrast, lactate and pyruvate of IRS-1 KO cells were not much different from those of WT cells in their isotopomer distributions, except for slightly higher M+1 isotopomer of pyruvate in IRS-1 KO cells.

#### C. Assessment of goodness of fit and flux estimation

In order to estimate the fluxes in the metabolic network of WT and IRS-1 KO cells on day 4 under 4 mM [U-<sup>13</sup>C] glutamine and 25 mM unlabeled glucose, the data for isotopomer distribution of nine metabolites (including palmitate) from WT and IRS-1 KO cells were plugged into the equations derived from the metabolic network (Fig. 5), using a MATLAB program designed for solving the equations with the measurements by least-square fit method (see “Experimental Procedures” for details).

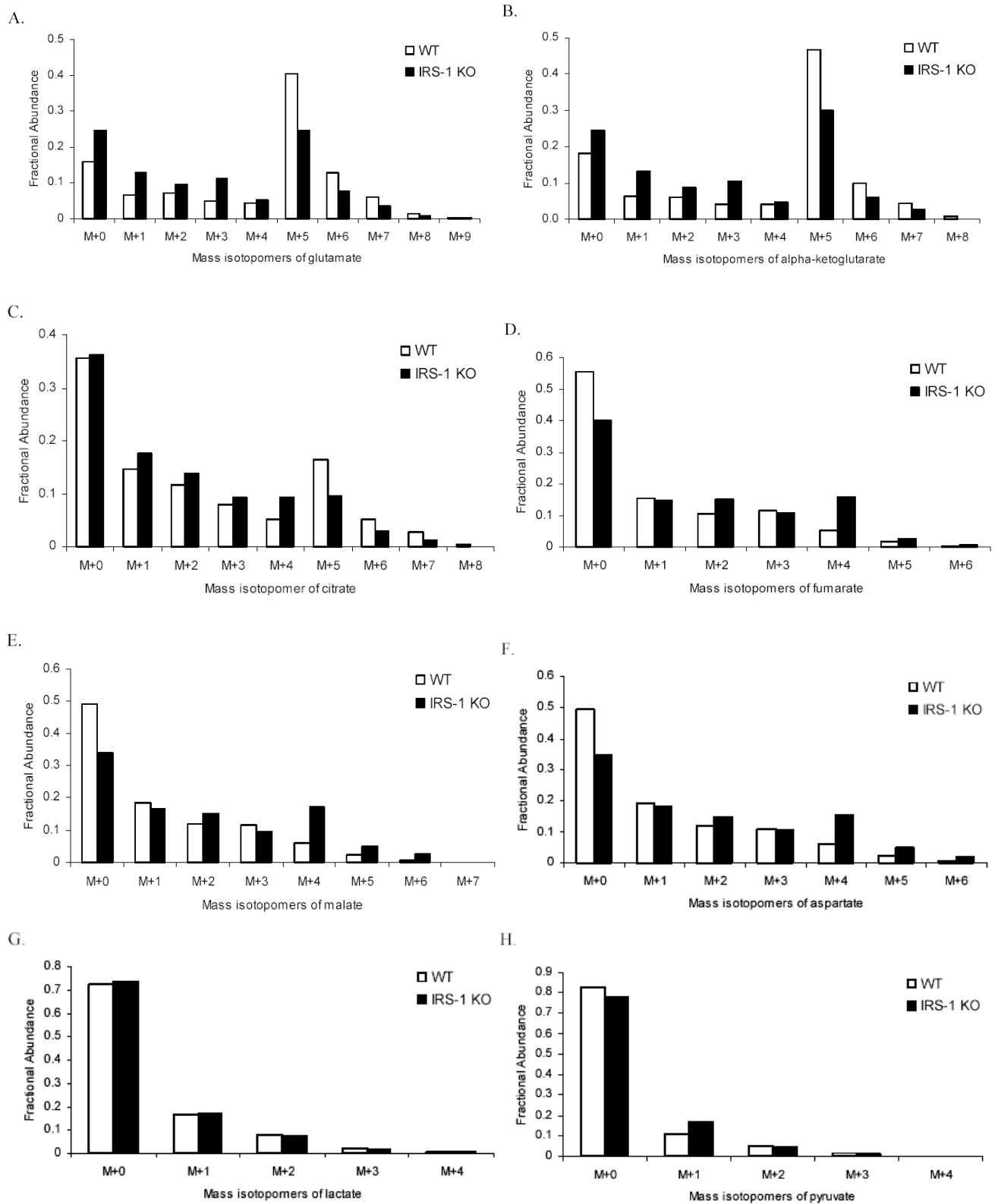


Fig. 4. Differential incorporation of glutamine carbon into some metabolites from WT and IRS-1 KO cells. Isotopomer distribution of glutamate(A), alpha-ketoglutarate (B), citrate (C), fumarate (D), malate(E), aspartate(F), lactate(G), and pyruvate(H) from WT and IRS-1 brown adipocytes on day 4 under 6-hr incubation in media containing 25 mM unlabeled glucose and 4 mM [ $U$ - $^{13}C$ ] glutamine. Data shown are mean  $\pm$  SEM (n = 3).

SSRES value of 56.656 (WT) and 60.294 (IRS-1 KO) were both within 95% confidence range of 26 – 62.

Uptake rate for glutamine and glucose into IRS-1 KO cells were measured and the relative uptake fluxes were set to be 100 for glutamine and 1100 for glucose. When absolute glutamine uptake rates from IRS-1 KO cells and WT cells were compared, the ratio was 40 to 100. Estimated fluxes for selected reactions in the metabolic network for IRS-1 KO cells are summarized in Figure 6, as compared with those for WT cells under the same experimental condition [12].

The relative flux of reductive carboxylation reaction was indistinguishable between WT and IRS-1 KO cells while that of the reverse reaction in IRS-1 KO cells was approximately 3-fold higher than in WT cells. This result led to net carbon flux of citrate to  $\alpha$ -ketoglutarate being  $128 \pm 4$  in IRS-1 KO cells, which was also added to make the flux of  $\alpha$ -ketoglutarate to succinate 6-fold higher in IRS-1 KO cells than in WT cells. Glycolytic fluxes were comparable between WT and IRS-1 KO cells until pyruvate was divided into dehydrogenation (AcCoA) or carboxylation (OAA). Pyruvate flux was heavily geared towards synthesis of acetyl-CoA in IRS-1 KO cells while it was more invested into carboxylation to oxaloacetate in WT cells. The flux of acetyl-CoA to palmitate synthesis was comparable between WT cells and IRS-1 KO cells, indicating relatively high activity of fatty acid synthase in IRS-1 KO cells. On the other hand, the flux of malate to pyruvate (catalyzed by malic enzyme) was 9-fold higher in WT cells than in IRS-1 KO cells.

#### IV. DISCUSSION

In order to investigate in detail the effect of insulin signaling on the lipogenic activity specifically involving glutamine's metabolic route to fatty acid synthesis, the fluxes of individual reactions related to the route were estimated through integration of isotopomer distribution data of nine metabolites from WT and IRS-1 KO brown adipocytes incubated with  $[U-^{13}C]$  glutamine. Since WT cells were shown to considerably employ reductive carboxylation pathway in their utilization of glutamine for fatty acid synthesis [7], the existence of the same pathway was first tested by measuring the incorporation of  $^{13}C$ -label from  $[5-^{13}C]$  glutamine into palmitate synthesis (Fig. 3). Although  $^{13}C$ -labeling on palmitate in IRS-1 KO cells was not as large as in WT cells, significant amount of  $^{13}C$  in palmitate from  $[5-^{13}C]$  glutamine indicated that reductive carboxylation pathway should be included in the metabolic network of IRS-1 KO cells.

When isotopomer distribution data for nine lipogenesis-related metabolites were compared between WT cells and IRS-1 KO cells under 6-hr incubation with 4 mM  $[U-^{13}C]$  glutamine, the general similarity of isotopomer patterns also suggested that WT and IRS-1 KO cells have the same metabolic network with different profile of individual fluxes (Figs. 4A-4I). M+5 isotopomers of glutamate,  $\alpha$ -ketoglutarate, and citrate were distinctively smaller in IRS-1 KO cells than in WT cells (Figs. 4A-4C). Because this isotopomer can originate from  $[U-^{13}C]$  glutamine only through reductive carboxylation pathway, the smaller peaks of M+5 isotopomer strongly indicates that IRS-1 KO cells

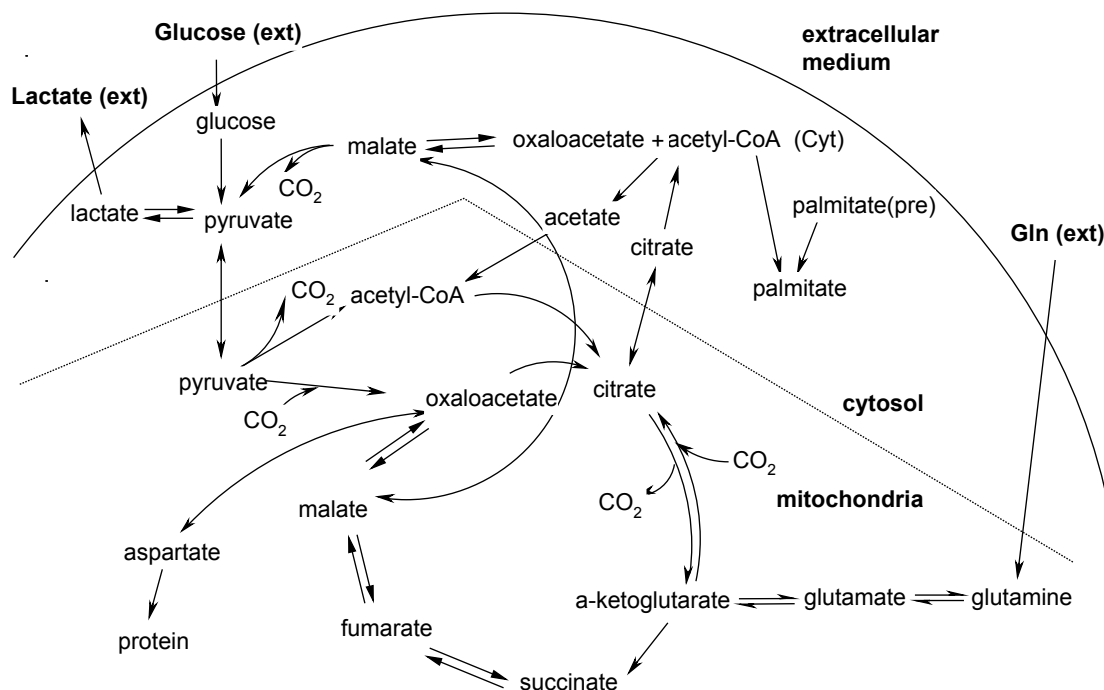


Fig. 5. Complete metabolic network model in steady state.

The model consists of glycolysis, fatty acid synthesis, and TCA cycle with glutamine entering at alpha-ketoglutarate via glutamate. For the steady-state metabolism, uptake of glucose and glutamine as well as pre-existing palmitate were regarded as inputs. Total palmitate, protein synthesis from aspartate, and lactate export were outputs. The rest of the metabolites were treated as balanced except for  $CO_2$ , which was allowed to be unbalanced.

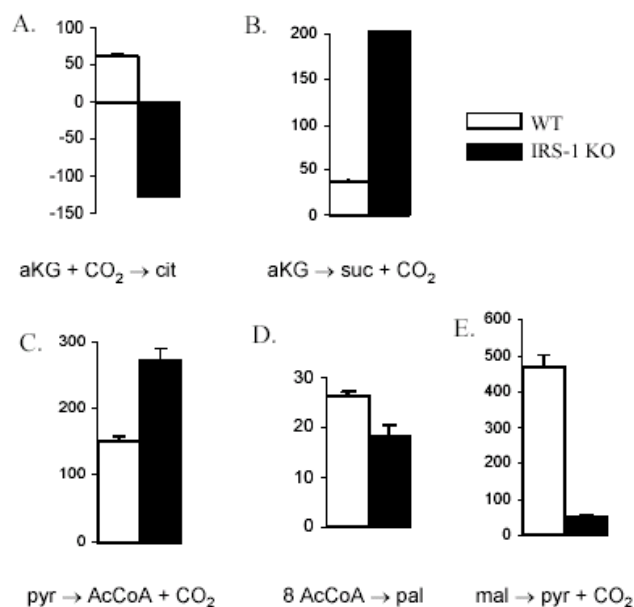


Fig. 6. Estimated fluxes for selected metabolic reactions in WT and IRS-1 KO brown adipocytes.

Estimated fluxes for  $\alpha$ -ketoglutarate to citrate (A: represented in net flux),  $\alpha$ -ketoglutarate to succinate (B), pyruvate to acetyl-CoA (C), acetyl-CoA to palmitate (D), and malate to pyruvate (E) in WT and IRS-1 KO brown adipocytes under incubation with 25 mM unlabeled glucose and 4 mM [U- $^{13}$ C] glutamine. Data shown are mean  $\pm$  SEM (n=3).

have relatively less activity of reductive carboxylation. On the other hand, a common feature of the isotopomer distributions of fumarate, malate, and aspartate from IRS-1 KO cells was greater abundance of M+4 isotopomer than in WT cells (Figs. 4D-4F). M+4 isotopomer can be derived from [U- $^{13}$ C] glutamine via direct conversion of  $\alpha$ -ketoglutarate to succinate, fumarate, malate, and oxaloacetate along the conventional direction of TCA cycle. Thus, greater abundance of M+4 isotopomer in fumarate, malate, and aspartate shows that IRS-1 KO cells have larger fluxes from  $\alpha$ -ketoglutarate to the direction of succinate than WT cells.

In order to integrate the isotopomer distribution of the metabolites (including palmitate) of IRS-1 KO cells into flux estimation, the same metabolic network as in WT cells were used. Overall goodness of fit for the flux estimation in terms of SSRES value fell within 95% confidence range of SSRES values, suggesting that this flux estimation is as close to reality as in WT cells. For the purpose of comparison between corresponding fluxes of WT and IRS-1 KO cells, uptake fluxes of glutamine and glucose in IRS-1 KO cells were set to be 100 and 1150 based on the measurement of consumption rate, although the absolute glutamine uptake in IRS-1 KO cells was only 40% of that in WT cells. Among all the estimated fluxes of WT and IRS-1 KO cells under standard condition, five fluxes were considered to be most meaningful for elucidating the fundamental difference in individual lipogenic fluxes (Fig. 6). Most distinctive was the net flux of  $\alpha$ -ketoglutarate to citrate, which was a large negative flux as opposed to the

positive net flux in WT cells. The limited contribution of reductive carboxylation pathway in IRS-1 KO cells as shown by [5- $^{13}$ C] glutamine experiment (Fig. 2) was overcome by large flux of TCA cycle in the conventional direction, which was also demonstrated by 6-fold higher flux of  $\alpha$ -ketoglutarate to succinate in IRS-1 KO cells. This result and the low D(glutamine) (fractional contribution of glutamine to lipogenic acetyl-CoA) of IRS-1 KO cells [7] indicates that the extent of glutamine's contribution to fatty acid synthesis depends more on the flux through reductive carboxylation pathway than the flux of conventional glutaminolysis pathway.

Relatively larger flux of pyruvate to acetyl-CoA in IRS-1 KO cells than in WT cells is consistent with D(glucose) (fractional contribution of glucose to lipogenic acetyl-CoA) in WT cells being significantly lower than that of IRS-1 KO cells [7] because conversion of pyruvate to acetyl-CoA is the first committed step for glucose flux to lipogenic acetyl-CoA pool. On the other hand, the relative extent of decrease in the flux of acetyl-CoA to palmitate (catalyzed by fatty acid synthase) due to absence of insulin signaling was not as significant despite the 9-fold smaller flux of malate to pyruvate via malic enzyme, which has been believed to heavily contribute to the supply of NADPH for fatty acid synthesis in brown adipose tissue [11].

Taken together, the low lipogenic activity in IRS-1 KO cells as shown by limited fat accumulation [7][9] was deconvoluted into differential contribution of individual fluxes related to the metabolic routes of glucose and glutamine to fatty acid synthesis. At least in brown adipocytes, lack of insulin signaling affected the lipogenic fluxes from glutamine to fatty acids to a greater degree than those from glucose to fatty acids. Decreased contribution of glutamine to fatty acid synthesis was mainly due to relatively smaller net flux of reductive carboxylation from  $\alpha$ -ketoglutarate to citrate. Thus, together with the results from previous studies [12], the present study revealed that reductive carboxylation through NADP-dependent isocitrate dehydrogenase can be a critical site of regulation for glutamine utilization in fatty acid synthesis of adipose cells and its activity can be manipulated either by hormone (insulin) or exogenous chemicals (specific inhibitors of NADP-ICDH).

#### ACKNOWLEDGMENT

WT and IRS-1 KO brown preadipocyte cell lines were generously provided by Dr. C. R. Kahn (Joslin Diabetes Center, Boston, MA, USA).

#### REFERENCES

- [1] C. T. Montague and S. O'Rahilly, "The perils of portliness: causes and consequences of visceral adiposity," *Diabetes*, vol. 49, pp. 883-8, 2000.
- [2] C. M. Nepokroeff, M. R. Lakshmanan, G. C. Ness, R. A. Muesing, D. A. Kleinsek, and J. W. Porter, "Coordinate

- control of rat liver lipogenic enzymes by insulin," *Arch Biochem Biophys*, vol. 162, pp. 340-4, 1974.
- [3] R. M. O'Brien and D. K. Granner, "Regulation of gene expression by insulin," *Physiol Rev*, vol. 76, pp. 1109-61, 1996.
- [4] J. M. Kowalchuk, R. Curi, and E. A. Newsholme, "Glutamine metabolism in isolated incubated adipocytes of the rat," *Biochem J*, vol. 249, pp. 705-8, 1988.
- [5] W. D. Reed, H. R. Zielke, P. J. Baab, and P. T. Ozand, "Ketone bodies, glucose and glutamine as lipogenic precursors in human diploid fibroblasts," *Lipids*, vol. 16, pp. 677-84, 1981.
- [6] A. L. Holleran, D. A. Briscoe, G. Fiskum, and J. K. Kelleher, "Glutamine metabolism in AS-30D hepatoma cells. Evidence for its conversion into lipids via reductive carboxylation," *Mol Cell Biochem*, vol. 152, pp. 95-101, 1995.
- [7] H. Yoo, G. Stephanopoulos, and J. K. Kelleher, "Quantifying carbon sources for de novo lipogenesis in wild-type and IRS-1 knockout brown adipocytes," *J Lipid Res*, vol. 45, pp. 1324-1332, 2004.
- [8] A. M. Valverde, M. Lorenzo, P. Navarro, and M. Benito, "Phosphatidylinositol 3-kinase is a requirement for insulin-like growth factor I-induced differentiation, but not for mitogenesis, in fetal brown adipocytes," *Mol Endocrinol*, vol. 11, pp. 595-607, 1997.
- [9] M. Fasshauer, J. Klein, K. M. Kriauciunas, K. Ueki, M. Benito, and C. R. Kahn, "Essential role of insulin receptor substrate 1 in differentiation of brown adipocytes," *Mol Cell Biol*, vol. 21, pp. 319-29, 2001.
- [10] O. Fiehn, J. Kopka, R. N. Trethewey, and L. Willmitzer, "Identification of uncommon plant metabolites based on calculation of elemental compositions using gas chromatography and quadrupole mass spectrometry," *Anal Chem*, vol. 72, pp. 3573-80, 2000.
- [11] J. Swierczynski, P. W. Scislowski, Z. Aleksandrowicz, and M. Zydowo, "Malic enzyme in brown adipose tissue-- purification, some properties and possible physiological role," *Int J Biochem*, vol. 13, pp. 365-72, 1981.
- [12] H. Yoo, M. Antoniewicz, J. K. Kelleher, and G. Stephanopoulos, "Quantitative analysis of individual carbon fluxes from glutamine to fatty acid synthesis in brown adipocytes", in preparation.